

available at www.sciencedirect.comjournal homepage: www.elsevier.com/locate/biochempharm

Inhibiting the function of ABCB1 and ABCG2 by the EGFR tyrosine kinase inhibitor AG1478

Zhi Shi^{a,b}, Amit K. Tiwari^a, Suneet Shukla^c, Robert W. Robey^d, In-Wha Kim^c, Smitaben Parmar^a, Susan E. Bates^d, Qiu-Sheng Si^e, Curtis S. Goldblatt^e, Ioana Abraham^a, Li-Wu Fu^{b,*}, Suresh V. Ambudkar^c, Zhe-Sheng Chen^{a,*}

^a Department of Pharmaceutical Sciences, College of Pharmacy and Allied Health Professions, St. John's University, Jamaica, NY 11439, USA

^b State Key Laboratory for Oncology in South China, Cancer Center, Sun Yat-Sen University, Guangzhou 510060, China

^c Laboratory of Cell Biology, Center for Cancer Research, NCI, NIH, Bethesda, MD 2089, USA

^d Medical Oncology Branch, Center for Cancer Research, NCI, NIH, Bethesda, MD 20892, USA

^e Department of Pathology, Conemaugh Memorial Medical Center, Johnstown, PA 15905, USA

ARTICLE INFO

Article history:

Received 9 October 2008

Accepted 10 November 2008

Keywords:

EGFR tyrosine kinase inhibitor

Multidrug resistance

ABCB1

ABCG2

ABSTRACT

The tyrphostin 4-(3-chloroanilino)-6,7-dimethoxyquinazoline (AG1478) is a potent and specific EGFR tyrosine kinase inhibitor (TKI); its promising pre-clinical results have led to clinical trials. Overexpression of ATP-binding cassette (ABC) transporters such as ABCB1, ABCC1 and ABCG2 is one of the main causes of multidrug resistance (MDR) and usually results in the failure of cancer chemotherapy. However, the interaction of AG1478 with these ABC transporters is still unclear. In the present study, we have investigated this interaction and found that AG1478 has differential effects on these transporters. In ABCB1-overexpressing cells, non-toxic doses of AG1478 were found to partially inhibit resistance to ABCB1 substrate anticancer drugs as well as increase intracellular accumulation of [³H]-paclitaxel. Similarly, in ABCG2-overexpressing cells, AG1478 significantly reversed resistance to ABCG2 substrate anticancer drugs and increased intracellular accumulation of [³H]-mitoxantrone as well as fluorescent compound BODIPY-prazosin. AG1478 also profoundly inhibited the transport of [³H]-E₂17βG and [³H]-methotrexate by ABCG2. We also found that AG1478 slightly stimulated ABCB1 ATPase activity and significantly stimulated ABCG2 ATPase activity. Interestingly, AG1478 did not inhibit the photolabeling of ABCB1 or ABCG2 with [¹²⁵I]-iodoarylazidoprazosin. Additionally, AG1478 did not alter the sensitivity of parental, ABCB1- or ABCG2-overexpressing cells to non-ABCB1 and non-ABCG2 substrate drug and had no effect on the function of ABCC1. Overall, we conclude that AG1478 is able to inhibit the function of ABCB1 and ABCG2, with a more pronounced effect on ABCG2. Our findings provide valuable contributions to the development of safer and more effective EGFR TKIs for use as anticancer agents in the clinic.

© 2008 Elsevier Inc. All rights reserved.

1. Introduction

The tyrphostin (tyrosine phosphorylation inhibitor) 4-(3-chloroanilino)-6,7-dimethoxyquinazoline (AG1478) is a low

molecular weight, highly potent, reversible, selective inhibitor of the epidermal growth factor receptor (EGFR, HER1/ErbB1) [1]. It not only competes with ATP at the ATP binding site of the kinase domain of EGFR, but also induces the formation of

* Corresponding authors. Tel.: +1 718 990 1432; fax: +1 718 990 1877.

E-mail addresses: Fulw@mail.sysu.edu.cn (L.-W. Fu), Chenz@stjohns.edu (Z.-S. Chen).

0006-2952/\$ – see front matter © 2008 Elsevier Inc. All rights reserved.

doi:10.1016/j.bcp.2008.11.007

inactive, unphosphorylated EGFR dimers in the presence and absence of ligand [2]. AG1478 inhibits the tyrosine kinase activity of EGFR with IC_{50} values in the nanomolar range [3], and its important chemical features for activity against EGFR include: the presence of electron-donating groups at positions 6 and 7 on the quinazoline; the presence of small lipophilic groups at position 3 of the aniline; and the orientation of the quinazoline ring nitrogens [4]. AG1478 is active in various types of cancer cell lines both *in vitro* and *in vivo*. In cell culture experiments, AG1478 demonstrates potent antiproliferative effects [5–7], and also enhances cellular sensitivity to cytotoxic drugs such as cisplatin, doxorubicin and etoposide [8,9]. In nude mouse tumor xenograft models, AG1478 directly inhibits the growth of human glioma xenografts that overexpress mutant EGFR ($\Delta 2$ -7 EGFR), and sensitizes these xenografts to the cytotoxicity of cisplatin and temozolomide; it also enhances the activity of the monoclonal antibody mAb 806 [10,11]. In addition, AG1478 enhances the efficacy of radio-immunotherapy with 90Y-CHX-A''-DTPA-hu3S193 in A431 squamous carcinoma cells nude mouse xenografts [12]. In a preclinical analysis, the initial pharmacokinetics and pharmacodynamics of AG1478 were evaluated in mice with novel AG1478 formulations in β -cyclodextrin (Captisol[®]) [13].

In this study, we investigated the effects of AG1478 on multidrug resistance (MDR)-linked ATP-binding cassette (ABC) transporters like ABCB1 (P-glycoprotein/P-gp, MDR1), ABCC1 (multidrug resistance protein 1, MRP1) and ABCG2 (breast cancer resistance protein, BCRP/MXR) in cancer cells. Our results show that AG1478 slightly reverses ABCB1-mediated MDR whereas it significantly inhibits ABCG2-mediated MDR by direct effect on drug efflux, but had no effect on ABCC1-mediated MDR.

2. Materials and methods

2.1. Reagents

[³H]-paclitaxel (37.9 Ci/mmol), [³H]-mitoxantrone (4 Ci/mmol) and [³H]-methotrexate (23 Ci/mmol) were purchased from Moravak Biochemicals Inc. (Brea, CA). [³H]-E₂17 β G (40.5 Ci/mmol) and [¹²⁵I]-Iodoarylazidoprazosin (IAAP) (2200 Ci/mmol) were obtained from PerkinElmer Life Sciences (Boston, MA). The fluorescent compound BODIPY-prazosin was purchased from Molecular Probes (Eugene, OR). Monoclonal antibodies C-219 (against ABCB1) and BXP-34 (against ABCG2) were acquired from Signet Laboratories Inc. (Dedham, MA). Anti-actin monoclonal antibody (sc-8432) was obtained from Santa Cruz Biotechnology Inc. (Santa Cruz, CA). Alexa flour 488 goat anti-mouse secondary antibody for immunocytochemistry was purchased from Molecular Probes (Eugene, OR). AG1478 was purchased from A.G. Scientific, Inc. (San Diego, CA). Fumitremorgin C (FTC) was synthesized by Thomas McCloud Developmental Therapeutics Program, Natural Products Extraction Laboratory, NCI, NIH (Bethesda, MD). Valspodar (PSC833) was obtained from Novartis Pharmaceuticals (East Hanover, NJ). A monoclonal anti-ABCB1 (MDR1) antibody (catalog no. P7965) and other chemicals were purchased from Sigma Chemical Co (St. Louis, MO).

2.2. Cell lines and cell culture

The ABCB1-overexpressing drug-resistant cell line KB-C2 was established by step-wise selection of the parental human epidermoid carcinoma cell line KB-3-1 in increasing concentrations of colchicine and was cultured in medium containing 2 μ g/ml of colchicines [14]. An ABCC1-overexpressing MDR cell line, KB-CV60, was also cloned from KB-3-1 cells and was maintained in medium with 1 μ g/ml of cepharanthine and 60 ng/ml of vincristine [15]. Both KB-C2 and KB-CV60 cell lines were kindly provided by Dr. Shin-ichi Akiyama (Kagoshima University, Japan). HEK293/pcDNA3.1, ABCG2-482-R5, ABCG2-482-G2, and ABCG2-482-T7 cells were established by selection with G418 after transfecting HEK293 with either empty pcDNA3.1 vector or pcDNA3.1 vector containing full length ABCG2 coding either arginine (R), glycine (G), or threonine (T) at amino acid 482, respectively, and were cultured in medium with 2 mg/ml of G418 [16]. All the cell lines were grown as adherent monolayers in flasks with DMEM culture medium (Hyclone Co., Omaha, NE) containing 10% bovine serum at 37 °C in a humidified atmosphere of 5% CO₂.

2.3. Preparation of membrane vesicles and total cell lysates

Membrane vesicles were prepared by the nitrogen cavitation method as previously described [17]. Vesicles were stored at –80 °C until ready for use. To prepare the total cell lysates, cells were harvested and rinsed twice with PBS. Cell extracts were prepared with RIPA buffer (1 \times PBS, 1% Nonidet P-40, 0.5% sodium deoxycholate, 0.1% SDS, 100 μ g/ml phenylmethylsulfonyl fluoride, 10 μ g/ml aprotinin, 10 μ g/ml leupeptin) for 30 min with occasional rocking followed by centrifugation at 12,000 g at 4 °C for 15 min. The supernatant containing total cell lysate was stored at –80 °C until ready for use. The protein concentration was determined by the Bradford method. High Five insect cells (Invitrogen, Carlsbad, CA) were infected with the recombinant baculovirus carrying the human MDR1 or ABCG2 cDNAs with a poly-His tag at the C-terminal end [BV-MDR1(His₆) or BV-ABCG2(His₁₀)] as described previously [18]. The membrane vesicles of High Five insect cells were prepared as previously described [19] and stored at –70 °C.

2.4. Western blot and immunocytochemistry analyses

Total cell lysate (50 μ g protein) or membrane vesicles (15 μ g protein) were resolved by SDS-PAGE and electrophoretically transferred onto polyvinylidene fluoride (PVDF) membranes. After incubating in blocking solution in TBST buffer (10 mM Tris-HCl, pH 8.0, 150 mM NaCl, and 0.1% Tween 20) for 1 h at room temperature, the membranes were first incubated overnight with primary monoclonal antibodies against ABCB1(C219) or actin at 1:200 dilution or ABCG2 at 1:500 dilution at 4 °C, and were then overnight at 4 °C with HRP-conjugated secondary antibody (1:1000 dilution). The protein-antibody complex was detected by chemoluminescence. The protein expression was quantified by Scion Image software (Scion Co., Frederick, MD). For immunocytochemistry analysis, cells (2×10^3) are seeded in 24 well plates, AG1478 at 10 μ M was added into the wells after overnight

culture. After 72 h of incubation, cells were washed with PBS and fixed with 4% paraformaldehyde for 15 min at room temperature and then rinsed with PBS three times. A monoclonal antibody against ABCB1 (1:500) (Sigma Chemical Co., St. Louis, MO) and a monoclonal antibody against ABCG2 (BXP-34, 1:200) were applied and incubated overnight, Alexa flour 488 goat anti-mouse IgG (1:1000, Molecular Probe, Carlsbad, CA) was added and cultured for 1 h. Propidium iodide was used for nuclear counterstaining. Immunofluorescence images were taken with an inverted microscope (model IX70; Olympus, Center Valley, PA) with IX-FLA fluorescence and CCD camera.

2.5. MTT cytotoxicity assay and colony formation assay

For MTT assay, cells were harvested with trypsin and resuspended at a final concentration of 4×10^4 cells/ml for KB-3-1 and 7.5×10^4 cells/ml for all the other cell lines. Aliquots (160 μ l) of each cell suspension were distributed evenly into 96-well multiplates. For reversal experiments, different concentrations of chemotherapeutic drugs (20 μ l/well) were added into designated wells after AG1478, verapamil, valspodar or FTC (20 μ l/well) was added. After 68 h of incubation, 20 μ l of 1-(4,5-dimethylthiazol-2-yl)-2,5-diphenyl tetrazolium bromide (MTT) solution (4 mg/ml) was added to each well, and the plate was further incubated for 4 h, allowing viable cells to change the yellow-colored MTT into dark-blue formazan crystals. Subsequently the medium was discarded, and 100 μ l of dimethylsulfoxide (DMSO) were added into each well to dissolve the formazan crystals. The absorbance was determined at 570 nm by an OPSYS microplate reader from DYNEX Technologies, Inc (Chantilly, VA). For colony formation assay, cells (1×10^3) were plated in 6-well plates in triplicate and culture overnight in DMEM medium. Different concentrations of AG1478 were added into designated wells next day. Cells were incubated for 10 days with one medium change and stained with Giemsa dye at room temperature for 30 min. Colonies were counted manually. For both MTT and colony formation assays, the concentrations required to inhibit growth by 50% (IC₅₀) were calculated from survival curves using the Bliss method [20].

2.6. Paclitaxel and mitoxantrone accumulation

The accumulation of paclitaxel in KB-3-1 and KB-C2 cells was measured using [³H]-paclitaxel as previously described [21], and the accumulation of mitoxantrone in ABCG2 related cells were measured using [³H]-mitoxantrone. Confluent cells in 24-well plates were preincubated with or without the reversing agents for 1 h at 37 °C. To measure drug accumulation, cells were then incubated with 0.1 μ M [³H]-paclitaxel or 0.2 μ M [³H]-mitoxantrone for 2 h in the presence or absence of the reversing agents at 37 °C. After washing three times with ice-cold PBS, the cells were trypsinized and lysed in 10 mM lysis buffer (pH 7.4, containing 1% Triton X-100 and 0.2% SDS). Each sample was placed in scintillation fluid and radioactivity was measured in a Packard TRI-CARB® 1900CA liquid scintillation analyzer from Packard Instrument Company, Inc (Downers Grove, IL).

2.7. Flow cytometry

Flow cytometry assays were performed as previously described [16]. Briefly, cells were trypsinized, resuspended in complete media (phenol red-free IMEM with 10% fetal calf serum) containing 250 nM BODIPY-prazosin alone or with various concentrations of the inhibitors for 30 min at 37 °C. Cells were then washed once in cold complete medium and then incubated for another 1 h at 37 °C in substrate-free media continuing with or without the described concentrations of the inhibitors to generate the efflux histograms. Subsequently, cells were washed twice with cold PBS and placed on ice at dark environment until ready for analysis. Cells were analyzed on a FACSort flow cytometer (BD, Franklin Lakes, NJ) equipped with a 488 nm argon laser. For all samples, at least 10,000 events were collected. Cell debris was eliminated by gating on forward vs side scatter, and dead cells were excluded based on propidium iodide staining.

2.8. In vitro transport assays

Transport assays were performed using the rapid filtration method as previously described [22]. Membrane vesicles were incubated with various concentrations of inhibitors for 1 h on ice, and then transport reactions were carried out at 37 °C for 10 min in a total volume of 50 μ l medium (membrane vesicles 10 μ g, 0.25 M sucrose, 10 mM Tris-HCl, pH 7.4, 10 mM MgCl₂, 4 mM ATP or 4 mM AMP, 10 mM phosphocreatine, 100 μ g/ml creatine phosphokinase, and 0.25 μ M [³H]-E₂17 β G or 0.5 μ M [³H]-methotrexate. Reactions were stopped by the addition of 3 ml of ice-cold stop solution (0.25 M sucrose, 100 mM NaCl, and 10 mM Tris-HCl, pH 7.4). During the rapid filtration step, samples were passed through 0.22 μ m GVWP filters (Millipore Corporation, Billerica, MA) presoaked in the stop solution. The filters were washed three times with 3 ml of ice-cold stop solution. Radioactivity was measured by the use of a liquid scintillation counter.

2.9. ATPase assay of ABCB1 and ABCG2

The Vi-sensitive ATPase activity of ABCB1 or ABCG2 in the membrane vesicles of High Five insect cells was measured as previously described [18]. The membrane vesicles (10 μ g of protein) were incubated in ATPase assay buffer (50 mM MES, pH 6.8, 50 mM KCl, 5 mM sodium azide, 2 mM EGTA, 2 mM dithiothreitol, 1 mM Ouabain, and 10 mM MgCl₂) with or without 0.3 mM vanadate at 37 °C for 5 min, then incubated with different concentrations of drugs at 37 °C for 3 min. The ATPase reaction was induced by the addition of 5 mM MgATP, and the total volume was 0.1 ml. After incubating at 37 °C for 20 min, the reactions were stopped by adding 0.1 ml of 5% SDS solution. The liberated P_i was measured as previously described [23]. In the inhibition assays, the Vi-sensitive ABCB1 or ABCG2 activity was measured in the presence of AG1478 alone or in combination with 50 μ M verapamil or 10 μ M FTC, respectively.

2.10. Photoaffinity labeling of ABCB1 and ABCG2 with [¹²⁵I]-IAAP

The photoaffinity labeling of ABCB1 and ABCG2 with [¹²⁵I]-IAAP was performed as previously described [24]. We used the

crude membranes from MCF7/Flv1000 cells expressing R482 ABCG2 and membrane vesicles from High Five insect cells expressing ABCB1 for photolabeling experiments. Membranes (50 μ g of protein) were incubated at room temperature with different concentrations of drugs in ATPase assay buffer with [125 I]-IAAP (7 nM) for 5 min under subdued light. The samples were photo-cross-linked by exposure to a 365 nm UV light for 10 min at room temperature. ABCG2 was immunoprecipitated using BXP21 antibody [23] while ABCB1 was immunoprecipitated as described previously except that C219 antibody was used [18]. The samples were subjected to SDS-PAGE in a 7% Tris-acetate NuPAGE gel, the gel was dried and exposed to Bio-Max MR film (Eastman Kodak Co., Rochester, NY) at -70°C for 8–12 h. The radioactivity incorporated into the ABCB1 or ABCG2 band was quantified using the STORM 860 Phosphor-Imager system and ImageQuANT (Molecular Dynamics, CA).

2.11. Statistical analysis

All experiments were repeated at least 3 times and the differences were determined by using the Student's *t*-test. The statistical significance was determined at $p < 0.05$.

3. Results

3.1. AG1478 sensitizes ABCB1- and ABCG2-overexpressing cells to chemotherapeutic drugs

AG1478 potently inhibits the growth of a wide range of cancer cell lines, and sensitizes cells to various chemotherapeutic drugs *in vitro* and *in vivo* [5–9]. But the effect of AG1478 on drug

resistant cancer cells, especially cells where MDR is mediated by ABC transporters, remains to be elucidated. To resolve this question, we first examined the sensitivity of ABCB1-, ABCC1-, and ABCG2-mediated MDR cells to AG1478. Interestingly, the results of the MTT assay showed that AG1478 did not inhibit the growth of any of the cell lines used in this study at concentrations up to 50 μM (Fig. 1A and C). As the MTT assay as an indirect measure of cytotoxicity, we conducted a colony formation assay to confirm the results of MTT assay. Our results again demonstrated that AG1478 itself exhibited low toxicity to the cell lines used and were consistent with those of MTT assay (Fig. 1B and D). The low cytotoxic potential of AG1478 may relate to the low or no expression of EGFR in the cell lines we used in this study. Higher AG1478 may be needed to kill these cell lines by other mechanisms than EGFR blockade, but these mechanisms are not yet fully understood. Next, we examined whether AG1478 could sensitize the MDR cells to chemotherapeutic drugs. As shown in Table 1, at a concentration of 10 μM , AG1478 slightly decreased the IC_{50} values for the ABCB1 substrates colchicine, vinblastine, and paclitaxel in the ABCB1-overexpressing KB-C2 cells, but did not alter the cytotoxicity of these chemotherapeutic drugs in parental KB-3-1 cells. Meanwhile, the known ABCB1 inhibitor verapamil at 10 μM completely reversed the resistance of KB-C2 cells to vinblastine, but only partially reversed resistance to colchicine, and paclitaxel (Table 1). We also used valsopodar at 5 μM to reverse ABCB1-mediated drug resistance, and the results showed that valsopodar almost completely reversed the resistance of KB-C2 cells to vinblastine, colchicine, and paclitaxel (Table 1). However, the IC_{50} values of another anticancer drug, cisplatin, which is not a substrate of ABCB1, were not affected by AG1478, verapamil or valsopodar in KB-3-1 and KB-C2 cells. Subsequently,

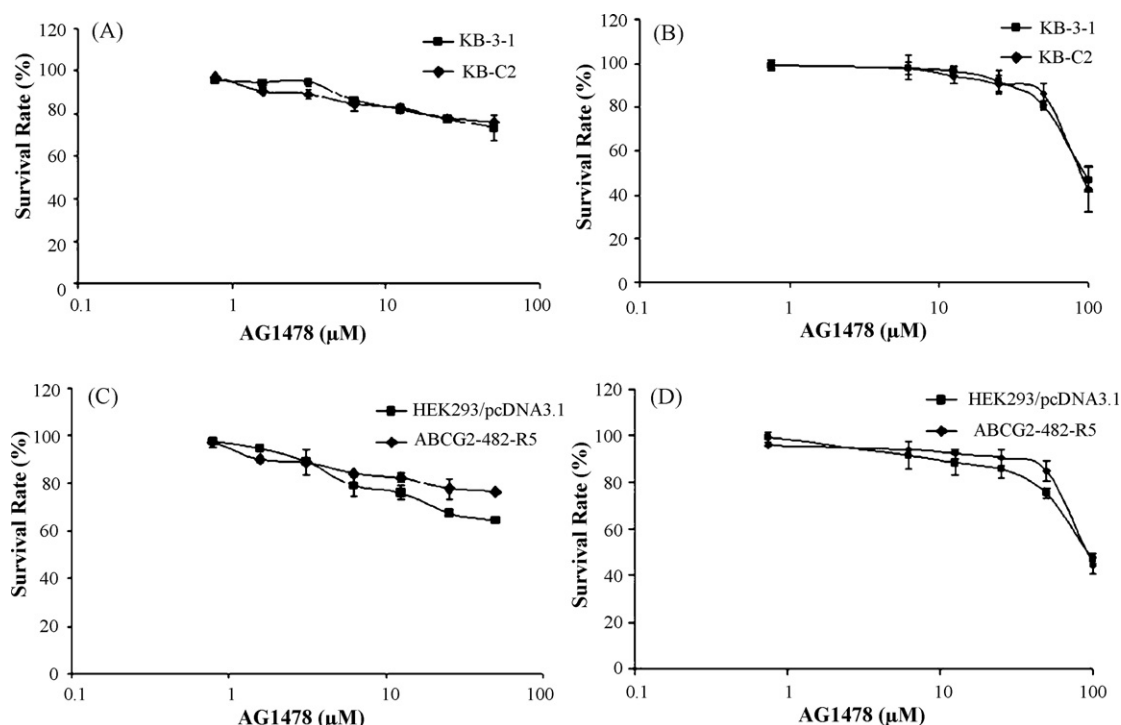


Fig. 1 – Effect of AG1478 on the survival of the overexpressing ABCB1 or ABCG2 cells. The results of MTT cytotoxicity (A and C) and colony formation assays (B and D) were used to measure cell survival as described in Section 2. Data points represent the means \pm SD of triplicate determinations. The representative results from three independent experiments are shown.

Table 1 – Effect of AG1478, verapamil and valsopodar on ABCB1-mediated resistance to colchicine, vinblastine, paclitaxel and cisplatin.^a

Compounds	IC ₅₀ ± SD (μM)	
	KB-3-1	KB-C2
Colchicine	0.0069 ± 0.0010(1.0) ^a	6.9543 ± 0.2437(947.8)
+ AG1478 10 μM	0.0069 ± 0.0004(1.0)	3.6490 ± 0.2268(505.8)
+ Verapamil 10 μM	0.0060 ± 0.0003(0.9)	0.1077 ± 0.0134(15.6)
+ Valsopodar 5 μM	0.0059 ± 0.0007(0.9)	0.0097 ± 0.0056(1.41)
Vinblastine	0.0476 ± 0.0043(1.0) ^a	0.3057 ± 0.0152(6.4)
+ AG1478 10 μM	0.0428 ± 0.0008(0.9)	0.1644 ± 0.0245(3.5)
+ Verapamil 10 μM	0.0408 ± 0.0062(0.9)	0.0419 ± 0.0078(0.9)
+ Valsopodar 5 μM	0.0389 ± 0.0045(0.8)	0.0399 ± 0.0098(0.8)
Paclitaxel	0.0084 ± 0.0023(1.0) ^a	5.5643 ± 1.1098(662.3)
+ AG1478 10 μM	0.0079 ± 0.0004(1.0)	1.4461 ± 0.2839(172.1)
+ Verapamil 10 μM	0.0072 ± 0.0018(0.9)	0.0173 ± 0.0077(2.0)
+ Valsopodar 5 μM	0.0068 ± 0.0021(0.8)	0.0093 ± 0.0064(1.1)
Cisplatin	1.8867 ± 0.0446(1.0) ^a	1.8235 ± 0.0782(1.0)
+ AG1478 10 μM	1.8365 ± 0.0578(1.0)	1.8293 ± 0.0811(1.0)
+ Verapamil 10 μM	1.8116 ± 0.0824(1.0)	1.7244 ± 0.0387(0.9)
+ Valsopodar 5 μM	1.8233 ± 0.0718(1.0)	1.8401 ± 0.0702(1.0)

To examine the effects of AG1478, verapamil and valsopodar on ABCB1-mediated resistance to colchicine, vinblastine, paclitaxel and cisplatin, cells were pre-incubated with or without AG1478, verapamil and valsopodar for 1 h and then incubated with various concentrations of colchicine, vinblastine, paclitaxel and cisplatin. Cell survival was determined by the MTT assay as described in Section 2. Data are means ± SD of at least three independent experiments performed in triplicate.

^a Fold-resistance was determined by dividing the IC₅₀ values of KB-C2 cells by the IC₅₀ values for KB-3-1 cells in the absence or presence of AG1478, verapamil or valsopodar.

the reversing effects of AG1478 on ABCC1- and ABCG2-mediated MDR were also determined. In the ABCC1-overexpressing KB-CV60 cells, AG1478 at 10 μM did not reduce the IC₅₀ value for vincristine, a known substrate of ABCC1 (data not shown). It has

been reported that mutations at amino-acid 482 in ABCG2 alter the substrate and antagonist specificity of ABCG2 [16,25], therefore we examined the reversing effect of AG1478 on both wild-type (R482) and mutant (R482G and R482T) ABCG2. As

Table 2 – Effect of AG1478 and FTC on ABCG2-mediated resistance to flavopiridol, mitoxantrone, SN-38 and cisplatin.^a

Compounds	IC ₅₀ ± SD (μM)			
	HEK293/pcDNA3.1	ABCG2-482-G2	ABCG2-482-R5	ABCG2-482-T7
Flavopiridol	0.1668 ± 0.0221(1.0) ^a	0.4132 ± 0.0465(2.4)	0.3127 ± 0.0265(1.9)	0.6968 ± 0.0571(4.2)
+ AG1478 2.5 μM	0.1637 ± 0.0134(1.0)	0.2339 ± 0.0333(1.4)	0.1855 ± 0.0293(1.1)	0.2797 ± 0.0258(1.7)
+ AG1478 10 μM	0.1662 ± 0.0161(1.0)	0.1959 ± 0.0182(1.2)	0.1696 ± 0.0046(1.0)	0.2415 ± 0.0547(1.5)
+ FTC 2.5 μM	0.1312 ± 0.0143(0.8)	0.1164 ± 0.0127(0.7)	0.1547 ± 0.0348(0.9)	0.1718 ± 0.0186(1.0)
Mitoxantrone	0.0323 ± 0.0021(1.0) ^a	1.2467 ± 0.0853(38.6)	0.4123 ± 0.0263(12.8)	0.7854 ± 0.1024(24.3)
+ AG1478 2.5 μM	0.0328 ± 0.0038(1.0)	0.2559 ± 0.0061(7.9)	0.0749 ± 0.0136(2.4)	0.2745 ± 0.1119(8.5)
+ AG1478 10 μM	0.0386 ± 0.0006(1.1)	0.1213 ± 0.0020(3.8)	0.0578 ± 0.0149(1.8)	0.1317 ± 0.0011(4.1)
+ FTC 2.5 μM	0.0302 ± 0.0034(0.9)	0.0611 ± 0.0016(1.9)	0.0446 ± 0.0087(1.4)	0.0867 ± 0.0102(2.7)
SN-38	0.0052 ± 0.0011(1.0) ^a	0.2234 ± 0.0863(43.0)	0.1446 ± 0.0562(22.0)	0.1004 ± 0.0082(19.3)
+ AG1478 2.5 μM	0.0050 ± 0.0004(1.0)	0.0336 ± 0.0013(6.5)	0.0286 ± 0.0035(5.5)	0.0217 ± 0.0003(4.2)
+ AG1478 10 μM	0.0048 ± 0.0002(0.9)	0.0137 ± 0.0006(2.6)	0.0150 ± 0.0032(2.9)	0.0091 ± 0.0005(1.7)
+ FTC 2.5 μM	0.0044 ± 0.0014(0.8)	0.0078 ± 0.0008(1.5)	0.0076 ± 0.0012(1.5)	0.0074 ± 0.0014(1.4)
Cisplatin	1.5466 ± 0.2489(1.0) ^a	1.4457 ± 0.1226(0.9)	1.4873 ± 0.3117(0.9)	1.6118 ± 0.1882(1.0)
+ AG1478 2.5 μM	1.6820 ± 0.0693(1.1)	1.2079 ± 0.2652(0.8)	1.1005 ± 0.2058(0.7)	1.6790 ± 0.2093(1.1)
+ AG1478 10 μM	1.3840 ± 0.2390(0.8)	1.1531 ± 0.3427(0.7)	1.1485 ± 0.0771(0.7)	1.5520 ± 0.0665(1.0)
+ FTC 2.5 μM	1.3347 ± 0.2586(0.8)	1.4632 ± 0.4487(0.9)	1.2256 ± 0.3251(0.8)	1.5671 ± 0.2641(1.0)

To examine the effects of AG1478 and FTC on ABCG2-mediated resistance to flavopiridol, mitoxantrone, SN-38 and cisplatin, cells were pre-incubated with or without AG1478 and FTC for 1 h and then incubated with various concentrations of flavopiridol, mitoxantrone, SN-38 and cisplatin. Cell survival was determined by the MTT assay as described in Section 2. Data are means ± SD of at least three independent experiments performed in trip.

^a Fold-resistance was determined by dividing the IC₅₀ values of the ABCG2-transfected cells by the IC₅₀ values of HEK293/pcDNA3.1 cells in the absence or presence of AG1478 or FTC.

shown in Table 2, in cells expressing either the wild-type or mutant ABCG2, AG1478 even at 2.5 μ M was able to moderately reverse resistance to flavopiridol, mitoxantrone, and SN-38, all of which are substrates of ABCG2. At a concentration of 10 μ M, AG1478 further sensitized the cells to these three drugs, and its efficacy was close to that of the known specific ABCG2 inhibitor FTC used at 2.5 μ M. However, in the parental cells HEK293/pcDNA3.1, the IC₅₀ values for flavopiridol, mitoxantrone or SN-38 in the presence or absence of AG1478 showed no significant difference. Similarly, the IC₅₀ values for cisplatin, not a substrate of ABCG2, were not affected by AG1478 or FTC in the four cell lines. Therefore, our results suggest that AG1478 selectively sensitizes ABCB1- or ABCG2-overexpressing cells to chemotherapeutic drugs which are the substrates of ABCB1 or ABCG2. AG1478 appeared to more specifically inhibit ABCG2-mediated resistance, as lower concentrations of AG1478 were required to inhibit ABCG2 than ABCB1.

3.2. AG1478 increases the accumulation of [³H]-paclitaxel in ABCB1 overexpressing cells, [³H]-mitoxantrone in the ABCG2 overexpressing cells

To investigate the potential mechanism by which AG1478 sensitizes ABCB1- and ABCG2-overexpressing cells to chemotherapeutic drugs, we examined the effect of AG1478 on the accumulation of chemotherapeutic drugs in ABCB1- or ABCG2-overexpressing cells. The intracellular [³H]-paclitaxel was measured in ABCB1-overexpressing cells in the presence or absence of AG1478, and the results are shown in Fig. 2A. The intracellular level of [³H]-paclitaxel in ABCB1-overexpressing KB-C2 cells were significantly lower than that of the parental KB-3-1 cells that do not express ABCB1. AG1478 at 10 μ M slightly increased the intracellular level of [³H]-paclitaxel in KB-C2 cells, but its effect was less pronounced than that of verapamil at 10 μ M. Neither AG1478 nor verapamil altered the intracellular levels of [³H]-paclitaxel in parental KB-3-1 cells. Similarly, the intracellular levels of [³H]-mitoxantrone were measured in the ABCG2-overexpressing cells in the presence or absence of AG1478 (Fig. 2B). The intracellular level of [³H]-mitoxantrone in cells expressing either wild type or mutant ABCG2 were significantly less than that in empty-vector transfected HEK293/pcDNA3.1 cells. In the presence of AG1478, either at 2.5 μ M or 10 μ M, all ABCG2-overexpressing cell lines displayed elevated intracellular [³H]-mitoxantrone levels, and intracellular levels of [³H]-mitoxantrone increased with increasing concentrations of AG1478. Furthermore, the effects of AG1478 at 10 μ M were slightly less than those observed for FTC at 2.5 μ M. Neither AG1478 nor FTC affected the intracellular levels of [³H]-mitoxantrone in HEK293/pcDNA3.1 cells.

3.3. AG1478 inhibits the ABCG2-mediated efflux of BODIPY-prazosin and transport of E₂17 β G and methotrexate

To assess the potency of AG1478 as an *in vitro* inhibitor of ABCG2, the ability of AG1478 to inhibit the transport activity of ABCG2 was analyzed using the chemotherapeutic drug substrate [³H]-methotrexate and the physiological substrate [³H]-E₂17 β G. In our previous study, only wild-type ABCG2 was shown being able to transport methotrexate and E₂17 β G in the *in vitro* transport system. Thus, we used membrane vesicles prepared from

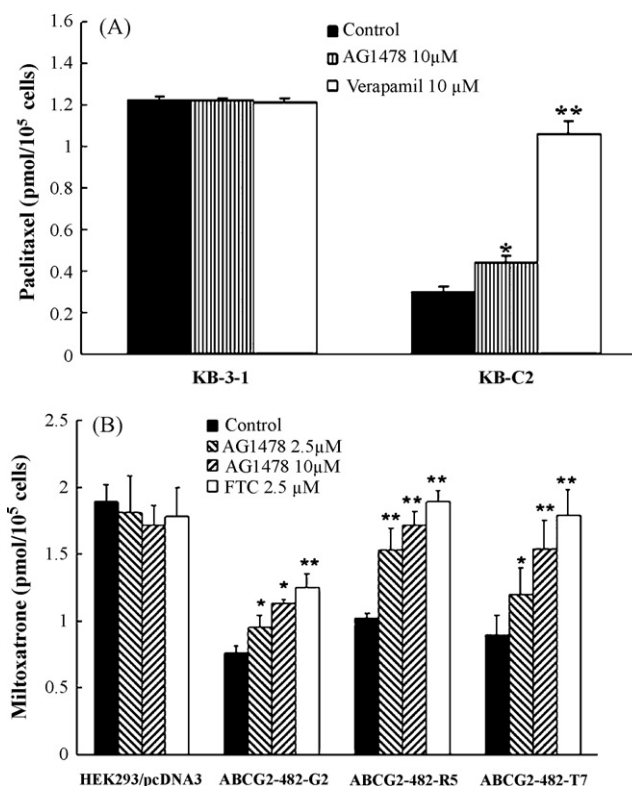


Fig. 2 – AG1478 increases the accumulation of [³H]-paclitaxel in ABCB1 overexpressing cells, [³H]-mitoxantrone in the ABCG2 overexpressing cells. The accumulation of [³H]-paclitaxel (A) or [³H]-mitoxantrone (B) was measured after cells were pre-incubated with or without AG1478, verapamil or FTC for 1 h at 37 °C and then incubated with 0.1 μ M [³H]-paclitaxel or 0.2 μ M [³H]-mitoxantrone for another 2 h at 37 °C. Data points represent the means \pm SD of triplicate determinations. **p* < 0.05 and *p* < 0.01, for values versus those in the control group. Independent experiments were performed at least three times, and a representative experiment is shown.**

HEK293/pcDNA3.1 and ABCG2-482-R5 cells (Fig. 3A). AG1478 significantly inhibited the rates of both methotrexate and E₂17 β G uptake in the membrane vesicles of ABCG2-482-R5 in a concentration-dependent manner, but its inhibitory effect was weaker than that of FTC at the same concentration. FTC also moderately decreased the rates of both methotrexate and E₂17 β G uptake in the membrane vesicles of HEK293/pcDNA3.1, while AG1478 did not. These *in vitro* transport results suggest that AG1478 is able to directly inhibit the transport of E₂17 β G and methotrexate by wild-type ABCG2.

In addition, we evaluated the effect of AG1478 on the ABCG2-mediated efflux of BODIPY-prazosin which is a known fluorescent substrate of ABCG2. AG1478 significantly inhibited the ABCG2-mediated efflux of BODIPY-prazosin in a concentration-dependent manner in the cells expressing either wild-type or mutant ABCG2. Representative histograms for BODIPY-prazosin are shown in Fig. 3B. The effect of AG1478 at 10 μ M was greater than that of AG1478 at 2.5 μ M, but weaker than that of FTC at 2.5 μ M. Taken together, these data suggest that AG1478 is

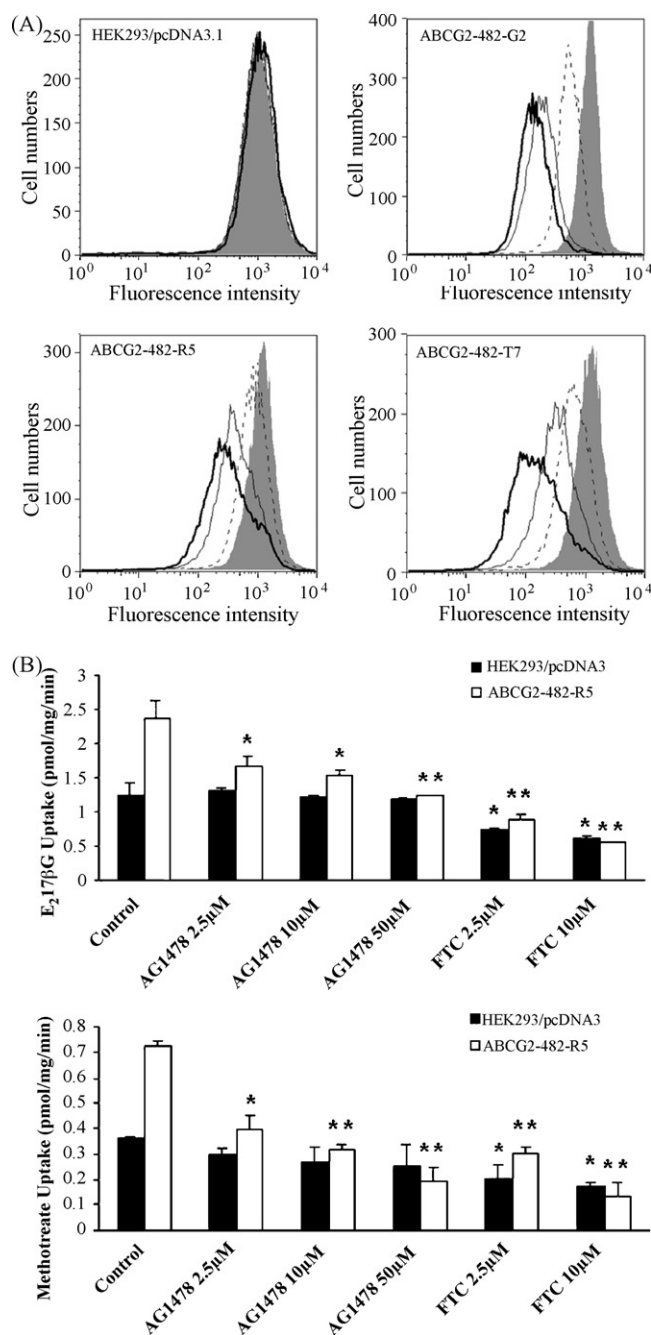


Fig. 3 – AG1478 inhibits the ABCG2-mediated efflux of BODIPY-prazosin and transport of E₂17βG and methotrexate. (A) Each cell lines were incubated in 250 nM BODIPY-prazosin alone (heavy solid line) or with 2.5 μM AG1478 (solid line), 10 μM AG1478 (dashed line) and 10 μM FTC (shaded histogram) for 30 min at 37 °C, after which the cells were washed, and allowed to efflux for 1 h at 37 °C in substrate-free media continuing with or without inhibitors. All samples were analyzed on a flow cytometer. **(B)** Membrane vesicles were prepared from HEK293/pcDNA3.1 and ABCG2-482-R5 cells. The rates of the uptake of [³H]-E₂17βG and [³H]-methotrexate into membrane vesicles (10 μg protein/reaction) with different concentrations of AG1478 and FTC were measured as described in Section 2. Data points represent the

able to inhibit the efflux function of ABCB1 and ABCG2 leading to the increase of intracellular accumulation of [³H]-paclitaxel in the ABCB1-overexpressing cells and [³H]-mitoxantrone as well as BODIPY-prazosin in the ABCG2-overexpressing cells.

3.4. AG1478 does not alter the expression or localization of ABCB1 and ABCG2

Reversal of ABCB1- and ABCG2-mediated MDR can be accomplished by either abrogating their activity, or decreasing ABCB1 and ABCG2 expression. To examine whether AG1478 affects the protein expression of ABCB1 and ABCG2, we treated KB-C2 and HEK293/ABCG2-482-R5 cells with AG1478 at 10 μM for 36 and 72 h. As shown in Fig. 4A, the protein levels of ABCB1 in KB-C2 cells and ABCG2 in HEK293/ABCG2-482-R5 cells were not altered in the presence of 10 μM of AG1478 when incubated with the drug for up to 72 h. Additionally, inhibition of AKT phosphorylation might cause the translocation of ABCG2 from the plasma membrane to the cytoplasm, leading to a reduction of functional ABCG2 molecules [26]. Since AG1478 may indirectly modulate phosphorylation status of AKT through EGFR or HER2, we also examined the location of ABCB1 and ABCG2 after AG1478 treatment. The results of immunocytochemistry experiments are shown in Fig. 4B, and there was no alteration of ABCB1 or ABCG2 protein expression in plasma membranes after cells were treated with AG1478 for 72 h. These results suggest that the reversal of ABCB1- and ABCG2-mediated MDR by AG1478 is not through altered expression or translocation of ABCB1 and ABCG2.

3.5. AG1478 activates the ATPase activity but does not affect the [¹²⁵I]-IAAP photo-labeling of ABCB1 and ABCG2

In general, most drugs known to be transported by ABCB1 stimulate ATPase activity, and among the reversal agents, some (e.g. verapamil) stimulate the activity whereas others (e.g. cyclosporin A) inhibit ATP hydrolysis [27]. To assess the effect of AG1478 on the ATPase activity of ABCB1 and ABCG2, the membrane vesicles of High Five insect cells which overexpress ABCB1 or ABCG2 were used to measure the ABCB1- and ABCG2-mediated ATP hydrolysis in the presence of various concentrations of AG1478 under conditions that suppressed the activity of other major membrane ATPases. As shown in Fig. 5A, AG1478 at the indicated concentrations mildly stimulated the ATPase activity of ABCB1, but potently stimulated the ATPase activity of ABCG2. The maximum stimulation of ATPase activities of ABCB1 and ABCG2 by AG1478 were up to 40–50% and 210–230%, respectively, and the concentration of AG1478 required for stimulating 50% of maximum ATPase activity of ABCB1 and ABCG2 were 3–5 μM and 0.2–0.3 μM, respectively. These data indicate that AG1478 may potentially be a weak substrate for ABCB1 compared to ABCG2. To determine the ability of AG1478 to interact with ABCB1 and ABCG2, we investigated the effect of verapamil at

means ± SD of triplicate determinations. **p* < 0.05 and ***p* < 0.01, for values versus those in the control group. At least three independent experiments were performed, and a representative experiment is shown.

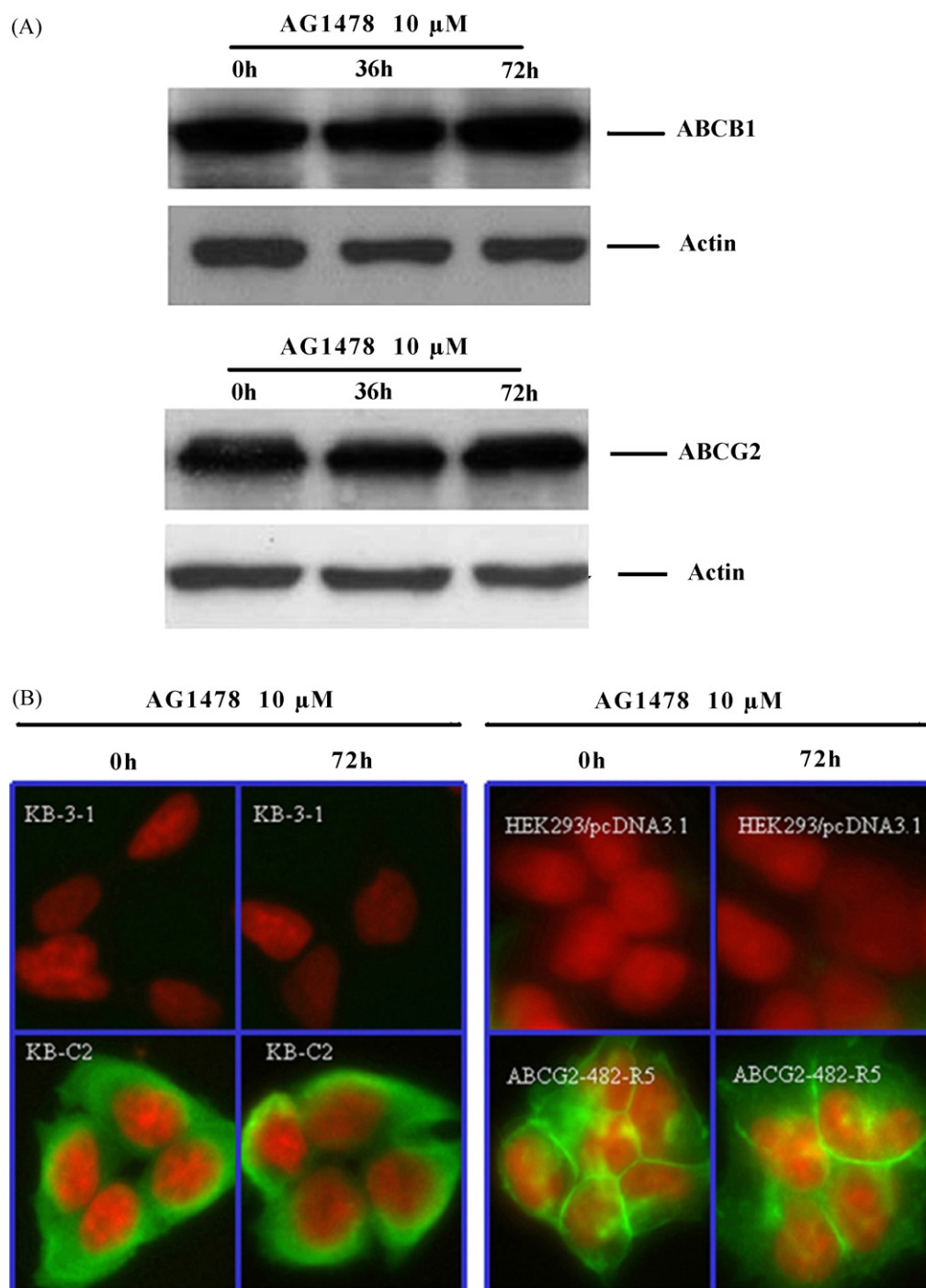


Fig. 4 – AG1478 does not affect the expression and localization of ABCB1 and ABCG2. (A) KB-C2 (upper panel) and HEK293/ABCG2-482-R5 (lower panel) cells were treated as indicated and Western Blot was performed. Results from a representative experiment are shown. Similar results were obtained in two other trials. (B) The localization of ABCB1 and ABCG2 by immunofluorescence was done on paraformaldehyde fixed cells using the indicated antibodies as outlined in Section 2. ABCB1 and ABCG2 specific staining is shown in green and the nuclear DNA stained by propidium iodide is shown in red. (For interpretation of the references to color in this figure legend, the reader is referred to the web version of the article.)

50 μ M or FTC 10 μ M on ATPase activity stimulated by AG1478. As shown in Fig. 5B, FTC at 10 μ M displayed direct inhibition of AG1478-activated ABCG2 ATPase activity (decreased from 61.6 ± 3.84 to 17.2 ± 2.22 nmoles P_i /mg protein/min). On the other hand, AG1478 had no significant effect on verapamil-

stimulated ABCB1 ATPase activity, (increased from 72.95 ± 6.50 to 86.76 ± 4.06 nmoles P_i /mg protein/min in the presence of 5 μ M AG1478 compared to 50 μ M verapamil alone).

The analogue of prazosin [125 I]-IAAP, which is able to bind to both ABCB1 and ABCG2 [23], has been widely used to

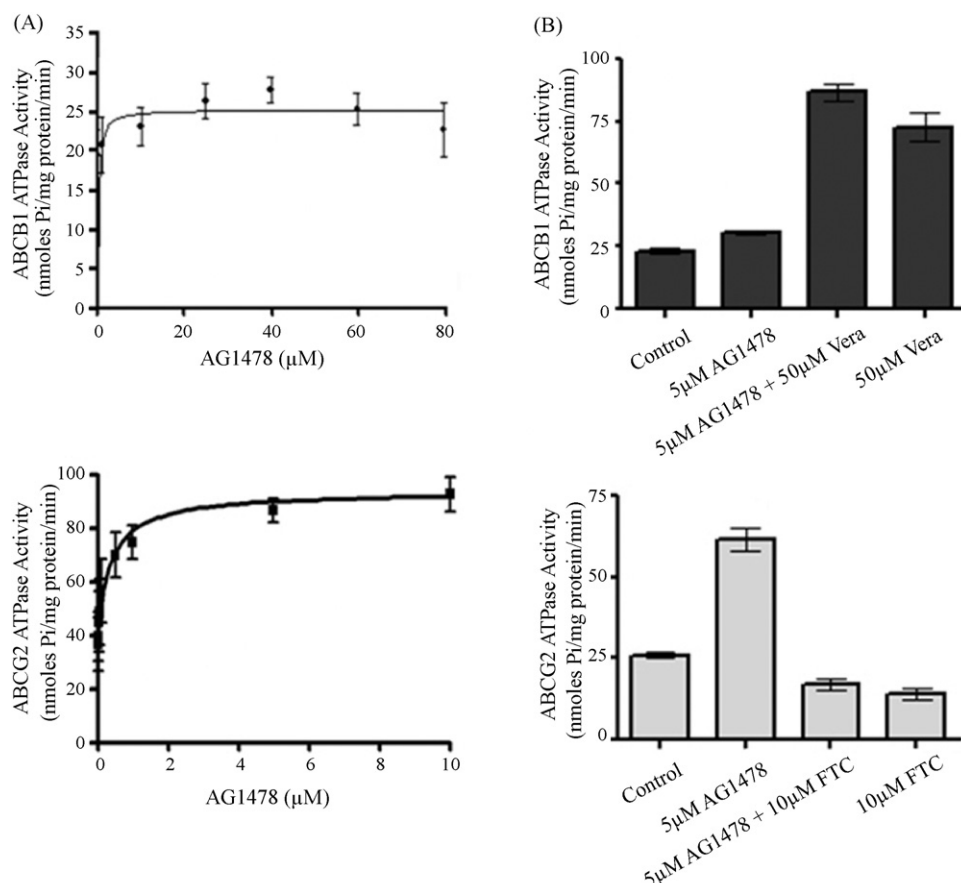


Fig. 5 – Effect of AG1478 with or without verapamil or FTC on the ATPase activity of ABCB1 and ABCG2. The Vi-sensitive ATPase activity of ABCB1 and ABCG2 with different concentrations of AG1478 (A), and in the presence of 5 μM AG1478, or 50 μM verapamil, or both together (for ABCB1), and 10 μM FTC (for ABCG2) alone or in combination with 5 μM AG1478 (B) were measured as described in Section 2. Mean values are given, and the error bars represent standard error from at least three independent experiments.

determine the regions of ABCB1 and ABCG2 that interact with substrates and inhibitors. To elucidate whether AG1478 interacts at the prazosin binding site of ABCB1 or ABCG2, the ability of AG1478 to prevent photolabeling of ABCB1 and ABCG2 with [125 I]-IAAP was examined by using the membrane vesicles from High Five insect cells transfected with ABCB1 or ABCG2. As indicated in Fig. 6A and B, AG1478 at 1–100 μM did not alter the photoaffinity labeling of ABCB1 or ABCG2 with [125 I]-IAAP. However, the ABCB1 substrates cyclosporine A at 10 μM and verapamil at 20 μM inhibited the [125 I]-IAAP photolabeling of ABCB1 up to ~95% and ~50% respectively, and the ABCG2 inhibitor FTC at 20 μM suppressed the [125 I]-IAAP photo-labeling of ABCG2 to ~50% compared to membranes incubated with no inhibitor. Thus, AG1478 at concentrations up to 100 μM does not affect the [125 I]-IAAP photolabeling of ABCB1 and ABCG2, suggesting that it binds to a separate site not shared by IAAP.

4. Discussion

In the present study, we are the first to report the effect of EGFR TKI AG1478 on ABCB1-, ABCC1- and ABCG2-mediated MDR in

cancer cells. Our data shows AG1478 had different effects on these three ABC transporters. Cytotoxicity assays showed that AG1478 mildly sensitized ABCB1 expressing cells to the substrates colchicine, vinblastine and paclitaxel; potentially sensitized wild-type or mutant ABCG2-overexpressing cells to the substrates flavopiridol, mitoxantrone and SN-38; but did not sensitize ABCC1-overexpressing cells to vincristine. Furthermore, AG1478 did not sensitize any of the cells examined to cisplatin and had no effect on the sensitivity of any of the parental cell lines (Tables 1 and 2). These data suggest that the reversing ability of AG1478 could be specific to ABCB1 and ABCG2, although AG1478 appeared to have greater affinity for ABCG2 than for ABCB1. Although AG1478 is known to inhibit phosphorylation of EGF receptor [2], this drug is not toxic to both sensitive (KB-3-1, HEK293) and drug resistant (KB-C2, HEK293/ABCG2-482-R5) cell lines (see Fig. 1A–D). These results clearly demonstrate that inhibition of EGF receptor function by AG1478 is not playing any role in reversal of drug resistance by AG1478 in drug resistant cell lines. Consistent with cytotoxicity data, the results of drug accumulation studies showed that AG1478 slightly enhances the intracellular accumulation of paclitaxel in the ABCB1 over-expressing cells, and significantly enhances the intracellular

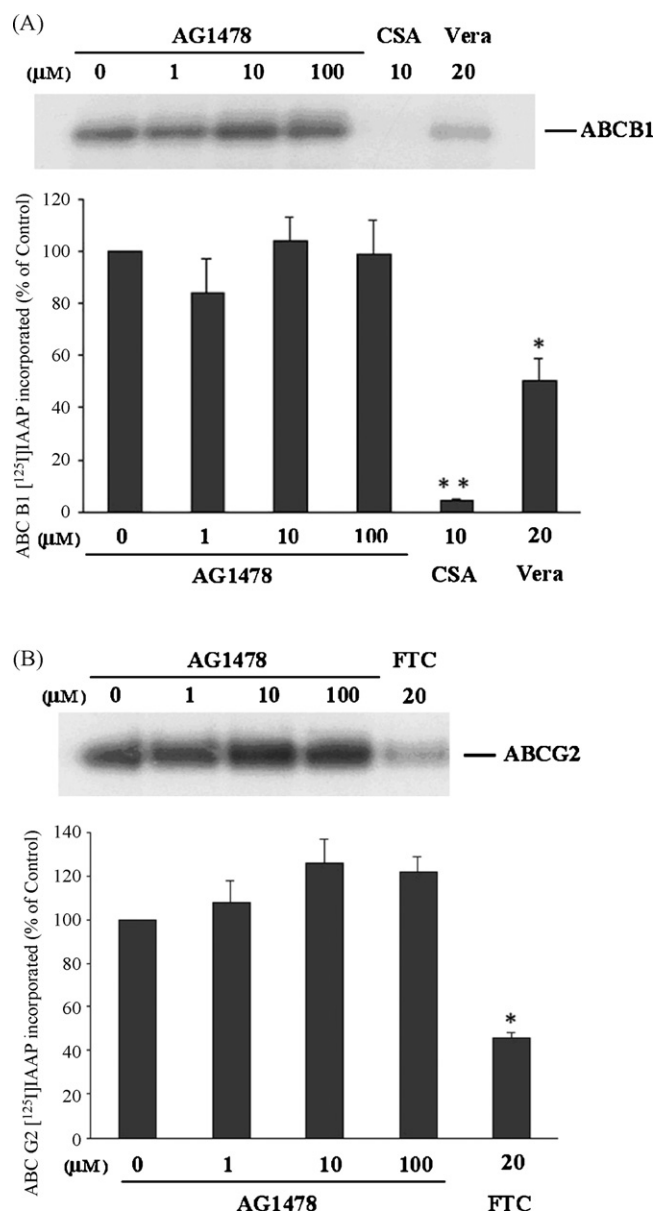


Fig. 6 – AG1478 does not affect the [¹²⁵I]-IAAP photoaffinity labeling of ABCB1 and ABCG2. The photoaffinity labeling of ABCB1 (A) and ABCG2 (B) with [¹²⁵I]-IAAP was performed as mentioned in Section 2. The lower panels show the quantify results from at least two independent experiments. Cyclosporine A, verapamil and FTC were used as positive controls. CSA: cyclosporine A; Vera: verapamil. * $p < 0.05$ and ** $p < 0.01$, for values versus those in the control group.

accumulation of mitoxantrone and BODIPY-prazosin in cells overexpressing either wild-type or mutant ABCG2. These results confirm that AG1478 has a greater affinity for ABCG2 than for ABCB1. In addition, the results of membrane vesicles transport experiments demonstrated that AG1478 directly inhibits ABCG2-mediated the transport of E₂17βG and methotrexate. The results of drug accumulation studies with whole cells and vesicles transport data indicate that AG1478 reverses

ABCB1- and ABCG2-mediated MDR by directly inhibiting the drug-transport function of ABCB1 and ABCG2. It has been reported that AG1478 can abolish the EGF-induced increase of ABCG2 at both the mRNA and protein levels [28]. Therefore, we examined the effect of AG1478 on ABCB1 and ABCG2 expression by treating ABCB1 or ABCG2-overexpressing cells with AG1478 at 10 μM for 36 and 72 h respectively, and the results showed that AG1478 did not alter the protein expression of ABCB1 and ABCG2 (Fig. 1C). In addition, there was no alteration of ABCB1 or ABCG2 protein expression in plasma membranes after treatment with AG1478 (Fig. 1D). Consequently, we infer that the mechanism by which AG1478 reverses ABCB1- and ABCG2-mediated MDR is through direct inhibition of drug transport activity. However, we cannot rule out the possibility that part of the reversing effect of AG1478 results from its effect on some proteins which may regulate the pump function of ABCB1 and ABCG2. Further experiments are needed to exclude this possibility. In addition, human P-glycoprotein is known to be phosphorylated by protein kinase A and protein kinase C and the phosphorylation sites are S661, S667, S671 and S683. By replacing S661, S667, S671 and S683 with either A or D, it has been shown that lack of phosphorylation of P-glycoprotein has no effect on the drug transport function of this transporter [29]. It is possible that phosphorylation may have some effect on the trafficking or stabilization of P-glycoprotein in mammalian cells but this needs to be studied further.

Additionally, in this study we also investigated the interaction between AG1478 and ABCB1 as well as ABCG2 by using the Vi (Vanadate)-sensitive ATPase assay and photoaffinity labeling with [¹²⁵I]-IAAP. Generally, the ATPase activity of ABC transporters is stimulated in the presence of transport substrates, and the fact that AG1478 mildly stimulated the ATPase activity of ABCB1 and powerfully stimulated the ATPase activity of ABCG2 suggests that it might potentially be a substrate of ABCB1 and ABCG2. Most reversing agents block drug transport by acting as competitive or noncompetitive inhibitors which bind either to drug interaction sites or to other modulator binding sites, leading to allosteric changes that prevent outward transport of drugs [27]. Hence, AG1478 may act as a competitive inhibitor of ABCB1 and ABCG2 by competing with drug substrates since AG1478 itself may be a substrate. Interestingly, when [¹²⁵I]-IAAP was used to photo-label ABCB1 and ABCG2, we found that AG1478 did not inhibit the photoaffinity labeling of ABCB1 and ABCG2 with [¹²⁵I]-IAAP (Fig. 4C and D). This indicates that AG1478 does not compete with IAAP for binding either to ABCB1 or ABCG2, suggesting that the binding sites of AG1478 on ABCB1 and ABCG2 may be distinct from that of IAAP. This finding is interesting and requires additional work.

Mechanistically, AG1478 shares the same structural quinazoline backbone with two clinically used EGFR TKIs gefitinib (Iressa, ZD1839) and erlotinib (Tarceva, OSI-774), but lacks the hydrophilic side chains that may confer significantly different properties [13]. The interaction of gefitinib with ABC transporters has been investigated by several groups. It has been reported that gefitinib is able to reverse ABCB1- and/or ABCG2-mediated MDR by directly inhibiting their drug pump function in cancer cells both *in vitro* and *in vivo* [30–36]. Furthermore, ABCG2-transduced cells were found to be resistant to gefitinib

[33], and expression of ABCG2, but not its nonfunctional mutant, protects EGFR signaling dependent tumor cells from death on exposure to gefitinib, and this protection was reversed by the ABCG2-specific inhibitor Ko143 [37]. These two reports strongly suggest that ABCG2 can actively pump gefitinib out from cells. In our previous study, we also found that erlotinib was also able to antagonize ABCB1- and ABCG2-mediated MDR, and might be the substrate of these two transporters [38]. When compared to erlotinib, the ability of AG1478 to reverse drug resistance and drug transport mediated by ABCB1 was weaker than that of erlotinib, but both of them had similar effects on ABCG2. The reason for the differential effects of AG1478 and erlotinib on the activity of ABCB1 may be related to the slight difference in the molecular structures of the two compounds, which becomes important when AG1478 and erlotinib interact with ABCB1. Based on the results of previous reports and the data presented here, it can be deduced that generally all quinazoline EGFR TKIs may interact with ABCB1 and ABCG2.

Currently, pre-clinical research and clinical trials are investigating the combination of EGFR TKIs with other anticancer drugs to improve the therapeutic outcome of cancer patients. Therefore, the interaction of EGFR TKIs with ABCB1 and ABCG2 should be addressed when exploring the combinational use of EGFR TKIs with cytotoxic anticancer drugs that are substrates of ABCB1 and ABCG2. Two important points should be considered. One is that EGFR TKIs may affect the pharmacokinetics of anticancer drugs, potentially resulting in increased responses but also potentially increasing adverse effects. This is especially true in the case of normal tissues and cancer tissues expressing a high level of ABCB1 and ABCG2, where the concentration and distribution of anticancer drugs might be altered. In fact, it has reported that when gefitinib was combined with camptothecins derivatives in mice, gefitinib was found to enhance the oral absorption of camptothecins, decrease the clearance of topotecan [32], increase the oral bioavailability of irinotecan [31], and increase the level of topotecan in brain extracellular fluid as well as decrease levels of topotecan in ventricular cerebrospinal fluid [39]. The other consideration is that the effect of EGFR TKIs might also be affected by the expression of ABCB1 and ABCG2. Recently, one common functional single-nucleotide polymorphism of ABCG2 Q141K (421C → A) was reported in association with gefitinib-induced diarrhea, and resulted in a high risk of diarrhea in patients treated with oral gefitinib [40]. The above group also indicated that this functional variant of ABCG2 was also associated with higher steady-state accumulation, toxicity and antitumor activity of gefitinib [41]. More recently, our group found that the EGFR and HER2/neu dual inhibitor Lapatinib reverses MDR in cancer cells *in vitro* and *in vivo* also by inhibiting the activity of ABCB1 and ABCG2 [42].

In conclusion, the present study demonstrates that AG1478 reverses ABCB1- and ABCG2-mediated MDR by directly inhibiting their drug efflux function, resulting in an increase of the intracellular concentration of anticancer drugs. Further study showed that AG1478 stimulated the ATPase activity of these two pumps but did not inhibit the photoaffinity labeling of the transporters with [¹²⁵I]-IAAP. Accordingly, the study of the interaction of EGFR TKIs with ABCB1 and ABCG2 presented

by us and other groups provide important clues leading to the development of safer and more effective EGFR TKIs in the future. A recent report showed that AG1478 enhances the efficacy of radioimmunotherapy with ⁹⁰Y-CHX-A''-DTPA-hu3S193 in A431 squamous carcinoma cells nude mouse xenografts without any sign of acute toxicity [12]. Whether AG1478 contributes to reversal of clinical resistance mediated by ABCB1 and/or ABCG2 remains to be determined. Analysis of reversal effect of AG1478 in tumor xenograft model should help to determine its importance in clinical drug resistance to cancer chemotherapy.

Acknowledgements

We thank Drs. Michael M. Gottesman (NCI, NIH, Bethesda, MD) for KB-3-1 cells, Shin-ichi Akiyama (Kagoshima University, Japan) for KB-C2 and KB-CV60 cell lines, Gary D. Kruh (Cancer Center, University of Illinois, Chicago, IL) for antibodies for ABCC subfamily members, Dong-Hua Yang (Robert Wood Johnson Medical School, New Jersey) for technical support of immunocytochemistry, Yangmin (Mimi) Chen (Montgomery High School, New Jersey) and Tong Shen (St. John's University, New York) for the editorial assistance. We thank Novartis Pharmaceuticals (East Hanover, New Jersey) for valspodar (PSC833). This work was supported by funds from St. John's University Tenure Track Faculty Start-Up Funding (No. C-0531, ZS. Chen), the Chinese Ministry of Education Doctor Foundation (No. 20050558062, L.W. Fu), and the Guangdong Provincial Key Sciences Foundation (No. 2004B30101005, L.W. Fu). I.W. Kim, S. Shukla, R.W. Robey, SE Bates and SV Ambudkar were supported by the Intramural Research Program, Center for Cancer Research, National Cancer Institute, NIH. Z. Shi is a recipient of Kaisi fellowship for overseas study at St. John's University from Sun Yat-Sen University.

REFERENCES

- Levitzki A, Gazit A. Tyrosine kinase inhibition: an approach to drug development. *Science* 1995;267:1782–8.
- Arteaga CL, Ramsey TT, Shawver LK, Guyer CA. Unliganded epidermal growth factor receptor dimerization induced by direct interaction of quinazolines with the ATP binding site. *J Biol Chem* 1997;272:23247–54.
- Gazit A, Chen J, App H, McMahon G, Hirth P, Chen I, et al. Tyrphostins IV—highly potent inhibitors of EGF receptor kinase. Structure-activity relationship study of 4-anilidoquinazolines. *Bioorg Med Chem* 1996;4:1203–7.
- Bridges AJ. The rationale and strategy used to develop a series of highly potent, irreversible, inhibitors of the epidermal growth factor receptor family of tyrosine kinases. *Curr Med Chem* 1999;6:825–43.
- Partik G, Hochecker K, Schorkhuber M, Marian B. Inhibition of epidermal-growth-factor-receptor-dependent signalling by tyrphostins A25 and AG1478 blocks growth and induces apoptosis in colorectal tumor cells *in vitro*. *J Cancer Res Clin Oncol* 1999;125:379–88.
- Shushan A, Rojansky N, Laufer N, Klein BY, Shlomai Z, Levitzki R, et al. The AG1478 tyrosine kinase inhibitor is an effective suppressor of leiomyoma cell growth. *Hum Reprod* 2004;19:1957–67.

- [7] Zhu XF, Liu ZC, Xie BF, Li ZM, Feng GK, Yang D, et al. EGFR tyrosine kinase inhibitor AG1478 inhibits cell proliferation and arrests cell cycle in nasopharyngeal carcinoma cells. *Cancer Lett* 2001;169:27–32.
- [8] Nagane M, Levitzki A, Gazit A, Cavennee WK, Huang HJ. Drug resistance of human glioblastoma cells conferred by a tumor-specific mutant epidermal growth factor receptor through modulation of Bcl-XL and caspase-3-like proteases. *Proc Natl Acad Sci U S A* 1998;95:5724–9.
- [9] Lei W, Mayotte JE, Levitt ML. Enhancement of chemosensitivity and programmed cell death by tyrosine kinase inhibitors correlates with EGFR expression in non-small cell lung cancer cells. *Anticancer Res* 1999;19:221–8.
- [10] Nagane M, Narita Y, Mishima K, Levitzki A, Burgess AW, Cavennee WK, et al. Human glioblastoma xenografts overexpressing a tumor-specific mutant epidermal growth factor receptor sensitized to cisplatin by the AG1478 tyrosine kinase inhibitor. *J Neurosurg* 2001;95:472–9.
- [11] Johns TG, Luwor RB, Murone C, Walker F, Weinstock J, Vitali AA, et al. Antitumor efficacy of cytotoxic drugs and the monoclonal antibody 806 is enhanced by the EGF receptor inhibitor AG1478. *Proc Natl Acad Sci U S A* 2003;100:15871–6.
- [12] Lee FT, Mountain AJ, Kelly MP, Hall C, Rigopoulos A, Johns TG, et al. Enhanced efficacy of radioimmunotherapy with 90Y-CHX-A''-DTPA-hu3S193 by inhibition of epidermal growth factor receptor (EGFR) signaling with EGFR tyrosine kinase inhibitor AG1478. *Clin Cancer Res* 2005;11:7080s–6.
- [13] Ellis AG, Doherty MM, Walker F, Weinstock J, Nerrie M, Vitali A, et al. Preclinical analysis of the analinoquinazoline AG1478, a specific small molecule inhibitor of EGF receptor tyrosine kinase. *Biochem Pharmacol* 2006;71:1422–34.
- [14] Akiyama S, Fojo A, Hanover JA, Pastan I, Gottesman MM. Isolation and genetic characterization of human KB cell lines resistant to multiple drugs. *Somat Cell Mol Genet* 1985;11:117–26.
- [15] Taguchi Y, Yoshida A, Takada Y, Komano T, Ueda K. Anti-cancer drugs and glutathione stimulate vanadate-induced trapping of nucleotide in multidrug resistance-associated protein (MRP). *FEBS Lett* 1997;401:11–4.
- [16] Robey RW, Honjo Y, Morisaki K, Nadjem TA, Runge S, Risbood M, et al. Mutations at amino-acid 482 in the ABCG2 gene affect substrate and antagonist specificity. *Br J Cancer* 2003;89:1971–8.
- [17] Cornwell MM, Gottesman MM, Pastan IH. Increased vinblastine binding to membrane vesicles from multidrug-resistant KB cells. *J Biol Chem* 1986;261:7921–8.
- [18] Ramachandra M, Ambudkar SV, Chen D, Hrycyna CA, Dey S, Gottesman MM, et al. Human P-glycoprotein exhibits reduced affinity for substrates during a catalytic transition state. *Biochemistry* 1998;37:5010–9.
- [19] Kerr KM, Sauna ZE, Ambudkar SV. Correlation between steady-state ATP hydrolysis and vanadate-induced ADP trapping in Human P-glycoprotein. Evidence for ADP release as the rate-limiting step in the catalytic cycle and its modulation by substrates. *J Biol Chem* 2001;276:8657–64.
- [20] Shi Z, Liang YJ, Chen ZS, Wang XW, Wang XH, Ding Y, et al. Reversal of MDR1/P-glycoprotein-mediated multidrug resistance by vector-based RNA interference in vitro and in vivo. *Cancer Biol Ther* 2006;5:39–47.
- [21] Aoki S, Chen ZS, Higasiyama K, Setiawan A, Akiyama S, Kobayashi M. Reversing effect of agosterol A, a spongian sterol acetate, on multidrug resistance in human carcinoma cells. *Jpn J Cancer Res* 2001;92:886–95.
- [22] Chen ZS, Robey RW, Belinsky MG, Shchavaleva I, Ren XQ, Sugimoto Y, et al. Transport of methotrexate, methotrexate polyglutamates, and 17 β -estradiol 17-(β -D-glucuronide) by ABCG2: effects of acquired mutations at R482 on methotrexate transport. *Cancer Res* 2003;63:4048–54.
- [23] Shukla S, Robey RW, Bates SE, Ambudkar SV. The calcium channel blockers, 1,4-dihydropyridines, are substrates of the multidrug resistance-linked ABC drug transporter, ABCG2. *Biochemistry* 2006;45:8940–51.
- [24] Sauna ZE, Ambudkar SV. Evidence for a requirement for ATP hydrolysis at two distinct steps during a single turnover of the catalytic cycle of human P-glycoprotein. *Proc Natl Acad Sci U S A* 2000;97:2515–20.
- [25] Honjo Y, Hrycyna CA, Yan QW, Medina-Perez WY, Robey RW, van de Laar A, et al. Acquired mutations in the MXR/BCRP/ABCP gene alter substrate specificity in MXR/BCRP/ABCP-overexpressing cells. *Cancer Res* 2001;61:6635–9.
- [26] Mogi M, Yang J, Lambert JF, Colvin GA, Shiojima I, Skurk C, et al. Akt signaling regulates side population cell phenotype via Bcrp1 translocation. *J Biol Chem* 2003;278:39068–75.
- [27] Ambudkar SV, Dey S, Hrycyna CA, Ramachandra M, Pastan I, Gottesman MM. Biochemical, cellular, and pharmacological aspects of the multidrug transporter. *Annu Rev Pharmacol Toxicol* 1999;39:361–98.
- [28] Meyer zu Schwabedissen HE, Grube M, Dreisbach A, Jedlitschky G, Meissner K, Linnemann K, et al. Epidermal growth factor-mediated activation of the map kinase cascade results in altered expression and function of ABCG2 (BCRP). *Drug Metab Dispos* 2006;34:524–33.
- [29] Germann UA, Chambers TC, Ambudkar SV, Licht T, Cardarelli CO, Pastan I, et al. Characterization of phosphorylation-defective mutants of human P-glycoprotein expressed in mammalian cells. *J Biol Chem* 1996;271:1708–16.
- [30] Nakamura Y, Oka M, Soda H, Shiozawa K, Yoshikawa M, Itoh A, et al. Gefitinib ("Iressa", ZD1839), an epidermal growth factor receptor tyrosine kinase inhibitor, reverses breast cancer resistance protein/ABCG2-mediated drug resistance. *Cancer Res* 2005;65:1541–6.
- [31] Stewart CF, Leggas M, Schuetz JD, Panetta JC, Cheshire PJ, Peterson J, et al. Gefitinib enhances the antitumor activity and oral bioavailability of irinotecan in mice. *Cancer Res* 2004;64:7491–9.
- [32] Leggas M, Panetta JC, Zhuang Y, Schuetz JD, Johnston B, Bai F, et al. Gefitinib modulates the function of multiple ATP-binding cassette transporters in vivo. *Cancer Res* 2006;66:4802–7.
- [33] Yanase K, Tsukahara S, Asada S, Ishikawa E, Imai Y, Sugimoto Y. Gefitinib reverses breast cancer resistance protein-mediated drug resistance. *Mol Cancer Ther* 2004;3:1119–25.
- [34] Yang CH, Huang CJ, Yang CS, Chu YC, Cheng AL, Whang-Peng J, et al. Gefitinib reverses chemotherapy resistance in gefitinib-insensitive multidrug resistant cancer cells expressing ATP-binding cassette family protein. *Cancer Res* 2005;65:6943–9.
- [35] Kitazaki T, Oka M, Nakamura Y, Tsurutani J, Doi S, Yasunaga M, et al. Gefitinib, an EGFR tyrosine kinase inhibitor, directly inhibits the function of P-glycoprotein in multidrug resistant cancer cells. *Lung Cancer* 2005;49:337–43.
- [36] Erlichman C, Boerner SA, Hallgren CG, Spieker R, Wang XY, James CD, et al. The HER tyrosine kinase inhibitor CI1033 enhances cytotoxicity of 7-ethyl-10-hydroxycamptothecin and topotecan by inhibiting breast cancer resistance protein-mediated drug efflux. *Cancer Res* 2001;61:739–48.
- [37] Elkind NB, Szentpetery Z, Apati A, Ozvegy-Laczka C, Varady G, Ujhelyi O, et al. Multidrug transporter ABCG2 prevents tumor cell death induced by the epidermal growth factor receptor inhibitor Iressa (ZD1839, Gefitinib). *Cancer Res* 2005;65:1770–7.
- [38] Shi Z, Peng XX, Kim IW, Shukla S, Si QS, Robey RW, et al. Erlotinib (Tarceva, OSI-774) antagonizes ATP-binding

- cassette subfamily B member 1 and ATP-binding cassette subfamily G member 2-mediated drug resistance. *Cancer Res* 2007;67:11012–20.
- [39] Zhuang Y, Fraga CH, Hubbard KE, Hagedorn N, Panetta JC, Waters CM, et al. Topotecan central nervous system penetration is altered by a tyrosine kinase inhibitor. *Cancer Res* 2006;66:11305–13.
- [40] Cusatis G, Gregorc V, Li J, Spreafico A, Ingersoll RG, Verweij J, et al. Pharmacogenetics of ABCG2 and adverse reactions to gefitinib. *J Natl Cancer Inst* 2006;98:1739–42.
- [41] Li J, Cusatis G, Brahmer J, Sparreboom A, Robey RW, Bates SE, et al. Association of variant ABCG2 and the pharmacokinetics of epidermal growth factor receptor tyrosine kinase inhibitors in cancer patients. *Cancer Biol Ther* 2007;6:432–8.
- [42] Dai CL, Tiwari AK, Wu CP, Su XD, Wang SR, Liu DG, et al. Lapatinib (Tykerb, GW572016) reverses multidrug resistance in cancer cells by inhibiting the activity of ATP-binding cassette subfamily B member 1 and G member 2. *Cancer Res* 2008;68:7905–14.